Mechanical and wear properties of Mg/Mo nanocomposites

M. John Iruthaya Raj[1], K. Manisekar[2], M. Gupta[3]*

[1] *School of Mechanical Engineering, Mar Ephraem College of Engineering and Technology, Malankara Hills, Elavuvilai 629 171, Tamil Nadu, India*
[2] *Department of Mechanical Engineering, National Engineering College, K. R. Nagar, Kovilpatti 628 503, Tamil Nadu, India*
[3] *Department of Mechanical Engineering, National University of Singapore (NUS), Singapore 117576, Singapore*

Abstract

This study investigates the microstructural, mechanical, and wear behaviour of magnesium/nano-molybdenum composites synthesized using microwave assisted powder metallurgy technique. Effects of varying amount of nano-sized molybdenum particles on magnesium matrix were studied. Microstructural studies of extruded nanocomposites exhibited a reasonably uniform distribution of molybdenum particles with the presence of minor clusters. Mechanical characterization of Mg/Mo nanocomposites showed improved hardness, tensile and compressive strengths while failure strain of magnesium matrix was adversely affected. Tensile fractured surfaces displayed the presence of micropores and microcracks while compressive fractured samples showed shear band formation. Results of sliding wear tests revealed that the increasing presence of nano Mo reinforcement reduced the wear rate. Worn surface of the composite specimens after the wear tests showed abrasion, delamination, oxidation, and adhesion as primary wear mechanisms.

K e y w o r d s: wear, microstructure, sintering, extrusion, characterization, nanocomposites, hardness, magnesium

1. Introduction

For an environmentally sustainable future, it is essential to reduce the weight of the structural materials used in weight-critical engineering applications such as in the transport sector. The significance of using lightweight materials in automobiles is quite evident because weight reduction reduces fuel consumption as well as carbon dioxide emission. Aluminium and its alloys are the incredibly beneficial and abundant group of materials used in various structural applications [1]. Magnesium-based materials have better weight reduction potential than most metals, and hence they are used as modern high performance, lightweight structural engineering materials for automotive, sports, electronics, and aerospace applications. Magnesium has many advantages, which include high specific strength, low density, exceptional castability, good machinability, stiffness, better damping characteristics, and excellent dimensional stability.

Among the reinforced metallic materials, magnesium-based composites provide an enormous potential to minimize energy consumption in a diverse range of engineering applications due to their superior specific mechanical properties. The plastic deformation in common engineering metals that have non-cubic crystal structures, such as magnesium, is more complicated than in cubic metals due to large plastic anisotropy and the presence of dislocation motion and twinning deformation. Limited ductility at room temperature, inferior fracture toughness, and reduced corrosion resistance limit the usage of Mg in many weight critical applications.

Many efforts have been focused by researchers to significantly enhance the combined strength and ductility level of pure magnesium, its alloys, and composites by reinforcing ceramic, metallic, and intermetallic particles of various sizes. Recent research findings have generally confirmed that the inclusion of reinforcement in the Mg matrix tends to enhance mecha-

nical properties like strength and ductility. The objective is to strongly disturb the motion of dislocations at each stage of deformation. The smaller in grain size of reinforcements lead to a reduction in mean travel distance of dislocations which activates the pile-up effect of dislocations at grain boundaries [2]. Hassan et al. [3] synthesized magnesium-based composite with copper as metallic reinforcement developed through liquid phase method and reported an improvement in hardness, stiffness, ultimate strength, and 0.2 % yield strength, however, ductility was adversely affected. Wong et al. [4] reported an improvement in elastic properties, hardness, 0.2 % offset yield strength, and UTS with the loss of failure strain in Mg/Cu nanocomposites processed through powder metallurgy technique. Zhong et al. [5] observed an overall improvement in strength characteristics by adding metallic aluminium nanoparticles to magnesium matrix processed through powder metallurgy route. Hassan et al. [6] in their study on titanium particle as reinforcement in magnesium matrix processed through the DMD process observed improvement of ductility and 0.2 % yield strength along with a marginal decrease in UTS.

The wear resistance, damping properties, and specific strength of matrix material can have a remarkable improvement by nanoparticles reinforcement. The inclusion of nanosized particles in magnesium matrix exhibited enhanced hardness, high specific strength, and wear properties without any meaningful change in ductility, making them inherently more resilient over Mg composites integrated with micron-size particles [7]. Molybdenum has a body-centered cubic crystalline structure with a high melting point of 2610 °C. Molybdenum is an alloying element in steels and cast irons to enhance hardness, toughness, strength at elevated temperatures and corrosion resistance. In earlier work, Wong et al. investigated the effect of the addition of micrometre size Mo, up to 3.6 % to pure magnesium using the DMD process [8]. However, no attempts have yet been reported so far to develop magnesium matrix composites containing nano-sized molybdenum particles through powder metallurgy route. Therefore, this study aimed to develop and characterize magnesium-based nanocomposites containing molybdenum nanoparticles using the powder metallurgy process.

2. Experimental procedures

2.1. Processing

The matrix material used in this study was magnesium metal powder (98.5 % purity, 60–300 μm, E. Merck, Germany). The metallic reinforcement was molybdenum nanopowder (99.8 % purity, 100 nm,

Sigma-Aldrich). Composite samples required were synthesized using Blend-Press-Sinter method incorporating Hybrid Microwave Sintering Technique [9]. For each composition, the weighed constituent powders were mixed entirely using a high energy ball mill (200 rpm/1 h). After thorough blending, the powders were cold compacted uniaxially using a servo-hydraulic press to produce a billet size of 35 mm in diameter and 40 mm in height. The green compacts were then coated with colloidal graphite and placed in a 900 W, 2.45 GHz IFB microwave oven for sintering [10]. The length of the sintering time was 23 min. For homogenization, the sintered compacts were kept in a muffle furnace under shielding gas environment for 1 h. The temperature maintained in the muffle furnace was 400 °C. The thermally homogenized compacts were then hot extruded by an extrusion ratio of 12.25 : 1 using a 200-ton hydraulic press at a temperature 350 °C. A rod of 10 mm diameter was obtained, and characterization studies were conducted on these rods.

2.2. Microstructural characterization

Microstructural analysis and the reinforcement distribution were carried out on lapped and acid-etched specimens acquired from the hot extruded composite materials. The metallographic analysis was performed using an Inverted Metallurgical Microscope (Model: Olympus GX51) equipped with a digital microscope camera. Mechanical polishing was performed using silicon carbide impregnated emery paper grades with 320-, 400-, 600-, 800-, and 1200-grit. Micro polishing was done using 1 μm alumina abrasive powder slurry as a lubricant. These polished cross-sectional samples were then etched by immersing in acetic picral solution to make the grain boundaries visible [11, 12]. Micrographs were taken using ZEISS EVO MA 25 Scanning Electron Microscope coupled with energy dispersion analysis (energy-dispersive spectroscopy). The X-ray diffraction (XRD) analysis of the polished samples from extruded pure magnesium and Mg-Mo nanocomposite samples was performed using Bruker D8 Advance diffractometer. XRD experimental conditions were: Cu Kα radiation generated at 40 kV and 40 mA, $\lambda = 1.5418$ Å.

2.3. Mechanical behaviour

The hardness was measured on polished surfaces of as-extruded samples. Microhardness measurements were performed on a Vickers micro-indentation hardness tester (Model: Shimadzu HMV-2TAW) as per ASTM E384-10. Macrohardness measurement was made by ASTM E18-15 using Rockwell Hardness Tester (FIE Model: RASN). Quasi-static tensile and compressive tests were carried out at room tempe-

T a b l e 1. Wear test conditions

Pin material	Pure Mg, Mg-0.3Mo, Mg-0.6Mo, Mg-1Mo
Disc material	Hardened EN-31 steel
Pin dimensions	Cylinder with diameter 6 mm and height 30 mm
Sliding speed (m s^{-1})	1.25
Normal load (N)	5, 10, 15, 20, 25
Sliding distance (m)	1000

rature using Universal Testing Machine (FIE Model: Unitek 94100) following ASTM standards. The dimensions of the tensile test specimen were prepared according to ASTM E8M-11. For compression test, cylindrical specimens with a gauge diameter of 8 mm and a gauge length of 8 mm (i.e., a length-to-diameter ratio of unity) were prepared according to Standard ASTM E9-09. Three samples were tested each for tensile and compressive testing to ensure repeatability. Fracture studies on the broken surfaces of the tensile and compressive loaded monolithic Mg and nanocomposite samples were accomplished using ZEISS EVO MA 25 scanning electron microscope equipped with energy dispersion spectroscopy analysis (EDS).

2.4. Wear behaviour

Dry sliding wear tests were conducted at room temperature as tabulated in Table 1 using DUCOM wear and friction monitor (DUCOM Instruments Pvt. Ltd, Bengaluru, India) model: ED – 201. The contact surfaces of the specimens were prepared perfectly smooth. The disc surface was ground using 600-grit SiC metallographic paper and then cleaned with acetone to remove the wear debris. The pin surface was prepared using an abrasive belt grinder mounted with 600-grit coated abrasive belt and then washed with acetone. The wear rates of the pins were determined using the weight loss method using a Shimadzu weighing balance AUX120 with an accuracy of 0.1 mg. On each specimen, three runs were made, and wear rate calculated with their average values. Worn surfaces and wear debris were characterized using ZEISS EVO MA 25 Scanning Electron Microscope.

3. Results and discussion

3.1. Microstructural characterization

Figure 1 shows the morphology and distribution of Mo reinforcement in the magnesium matrix. It was noticed that Mo nanoparticles were uniformly distributed throughout the matrix; however, as the Mo content increased, the increasing presence of clusters in the matrix was evident as displayed in Fig. 2. The number of clusters and agglomerates appears to be more in the composites containing 0.6 and
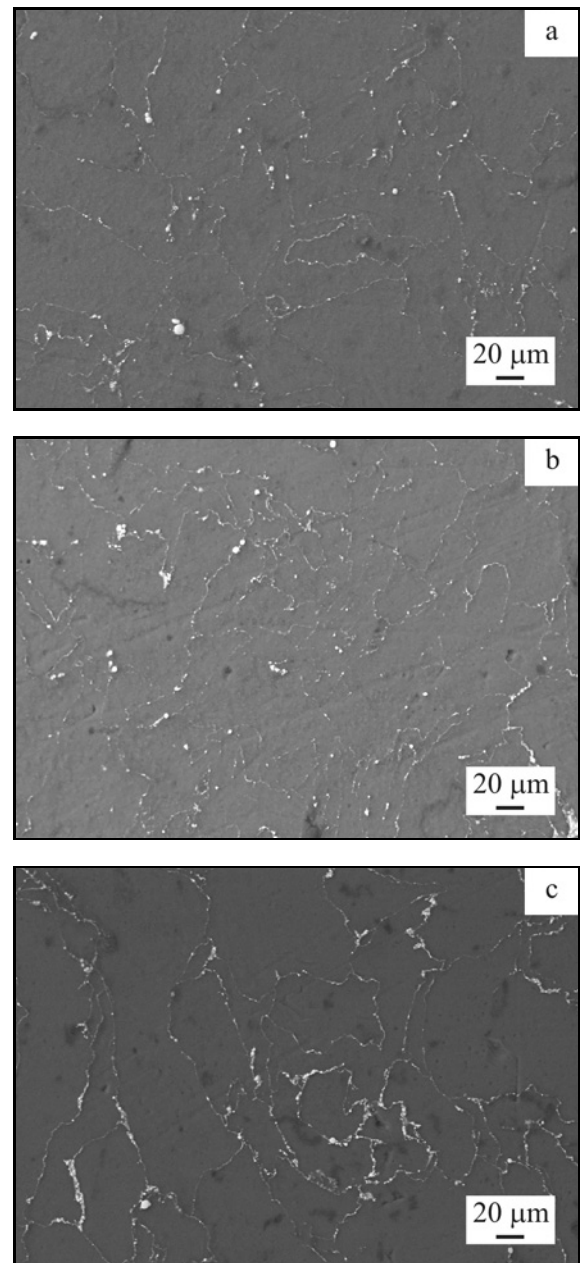

Fig. 1. SEM images showing the distribution of Mo nanoparticles through the Mg matrix in the case of (a) Mg/0.3Mo, (b) Mg/0.6Mo, and (c) Mg/1.0Mo nanocomposites.

1 vol.% nano Mo than in the composite with 0.3 vol.% Mo. The increasing tendency of agglomeration of

T a b l e 2. Results of grain size measurements

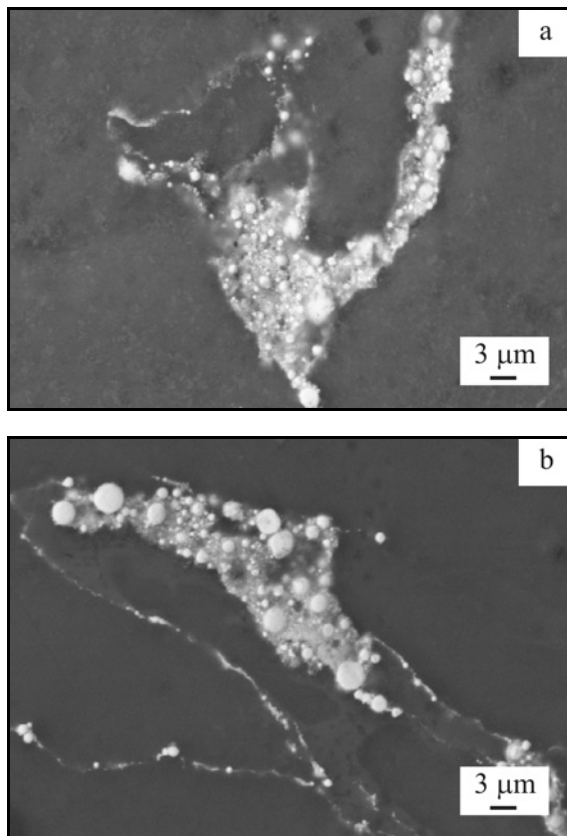| S. No.	Material	Grain size (μm)
1	Pure Mg	27 ± 9
2	Mg-0.3Mo	26 ± 6
3	Mg-0.6Mo	27 ± 9
4	Mg-1Mo	29 ± 7

Fig. 2. SEM images showing the presence of Mo cluster in the case of (a) Mg/0.6Mo and (b) Mg/1.0Mo nanocomposites.

the nanoparticles can be attributed to the high surface energy and a large specific surface area possessed by the nanometric reinforcement [13]. The results indicated that the distribution of nano-length scale particles becomes more challenging with the increase in their amount. The nanoparticles aggregation/agglomeration in the magnesium matrix would deteriorate the mechanical properties of the composite. The well-dispersed state of nano-reinforcements is significant to realize superior physical and mechanical properties of the composites. The results thus suggested that further optimization of blending parameters is needed mainly for higher volume percentage of Mo particles. Another probable reason for clustering is the vast difference in size of Mo particles (100 nm) and micron-sized Mg particles (60–300 μm) [14]. Pre-

vious studies have also shown that the agglomeration can offer strength to the composites if they are bonded well with the matrix [15]. The dispersion of nanoparticles in the magnesium matrix was uniform, and the densification capacity of the composites improved by nanoparticle-clusters filled the voids between the matrix particles.

The microstructure analysis of Mo nanoparticle reinforced Mg composites indicated the presence of near-equiaxed grain morphology. The grain size remains essentially unchanged up to 0.6 % of Mo reinforcement as shown in Table 2. These results showed the inability of nano Mo particles to change grain size within the reinforcement amount limited to 1 % [16]. The failure of grain size refinement by nano Mo particles may also be partially attributed to the increasing presence of Mo clusters with the increasing presence of Mo in the matrix. It is apparent that poor grain refinement also supported by the highest average grain size exhibited by Mg-1Mo composite sample. For magnesium-based materials, control of grain refinement can also be attained by hot extrusion, resulting in significant improvement of mechanical properties [17]. The grain size refined by dynamic recrystallization during the hot extrusion process indicated that nanoparticle agglomerates suppressed a grain growth during hot extrusion. The XRD results (Fig. 3) of all samples exhibited the presence of peaks related to Mg. The XRD experiment did not detect Mo, MgO, and any other related phases. These observations suggest that within the XRD resolution limit it is difficult to identify a relatively low volume percentage and small size of reinforcements [18]. XRD results also indicate that basal texture dominates in both monolithic and composite samples. In particular, the intensity of peak corresponding to pyramidal plane exhibited higher intensity when compared to the monolithic sample in all composite samples indicating that Mo particles as reinforcement play a definitive role in randomizing the texture.

3.2. Mechanical behaviour

The results obtained from hardness measurements in Table 3 revealed that the addition of nano Mo reinforcement caused minimal changes in the macrohardness and significant improvement in microhardness values of the composites. The microhardness values
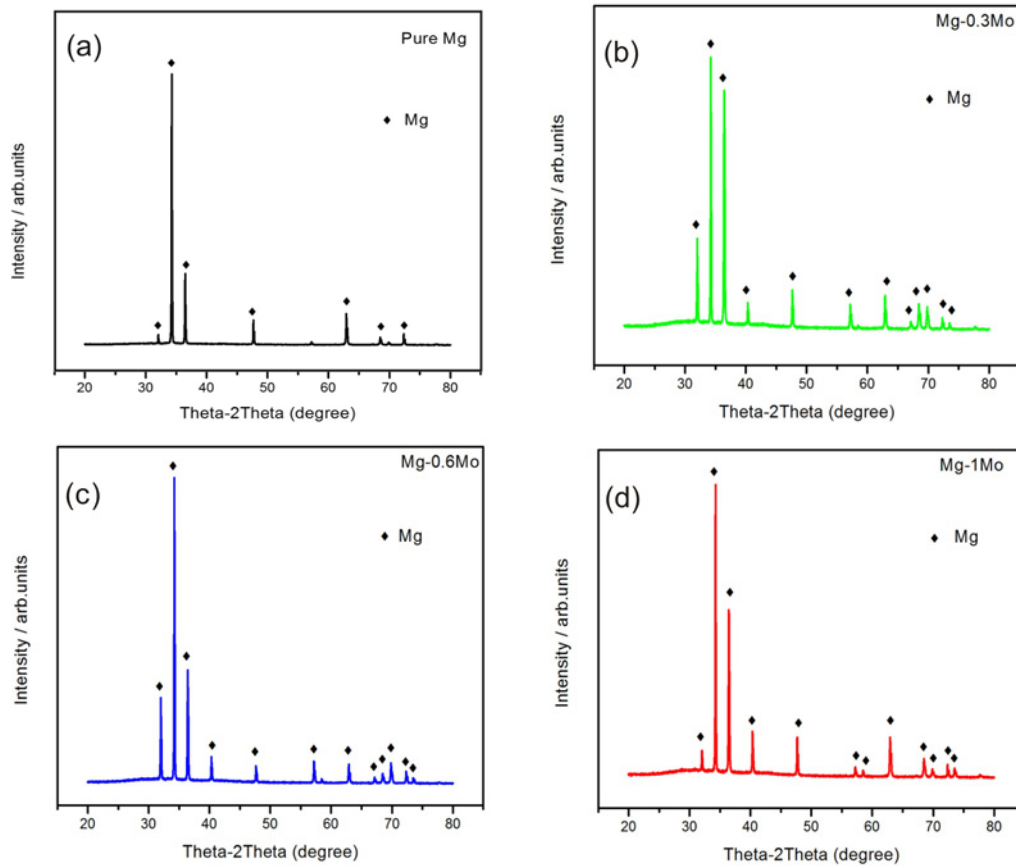
Fig. 3. X-ray diffraction traces obtained from developed Mg/Mo nanocomposites.

T a b l e 3. Results of hardness measurements

Materials	Macrohardness, HR15T	Vickers microhardness, HV
Pure Mg	47 ± 1	39 ± 1
Mg-0.3Mo	47 ± 1	44 ± 1
Mg-0.6Mo	48 ± 1	44 ± 1
Mg-1Mo	48 ± 1	46 ± 2 (18 % improvement)

visibly improved due to the presence of Mo nanoparticles and 18 % improvement was realized in the case on Mg-1Mo composite. The higher number of nanoparticles in the magnesium matrix could further promote dislocations resulting improvement in microhardness values. These observations are also consistent with the remarks made by researchers elsewhere [19, 20].

Figure 4 and Table 4 summarize tensile characteristics such as yield stress, ultimate tensile strength, and failure strain of the samples with various volume percentages of Mo nanoparticles. Both average tensile and yield strengths of composites were improved marginally by the increasing presence of Mo nanoparticles when compared to monolithic Mg. The nanocomposite which contains 1 volume percentage of Mo displayed more significant improvement with an increase in ∼ 7 % of 0.2 % YS, and ∼ 11 % in UTS.

The significant increase in strength levels may be attributed to the positive influence of the distribution of particles, good matrix-reinforcement interfacial bonding, increased density of dislocations, and the negative impact of particle agglomeration [21]. The results further showed that the addition of nanosized molybdenum particulates was more effective in improving the elastic modulus of magnesium. In reinforced metal matrix composites, active load transfer from matrix to reinforcement additionally strengthens the resulting composite. The tensile test results also indicate a marginal decrease in the failure strain of composite samples. The drop-in failure strain may primarily be attributed to the presence of clusters that are capable of triggering grain boundary cavitation due to the intense concentration of internal stresses in the cluster under tensile loading.

T a b l e 4. Results of room temperature tensile properties

Material	0.2% YS (MPa)	UTS (MPa)	Failure strain (%)
Pure Mg	109 ± 7	171 ± 13	6.8 ± 0.7
Mg-0.3Mo	112 ± 9	172 ± 10	3.9 ± 0.3
Mg-0.6Mo	116 ± 8	183 ± 15	6.1 ± 0.5
Mg-1Mo	117 ± 6	190 ± 11	4.3 ± 0.6

T a b l e 5. Results of room temperature compressive properties

Material	0.2% CYS (MPa)	UCS (MPa)	Failure strain (%)
Pure Mg	67 ± 7	252 ± 6	17.3 ± 0.5
Mg-0.3Mo	73 ± 4	259 ± 8	12.7 ± 0.7
Mg-0.6Mo	73 ± 3	268 ± 9	12.0 ± 0.4
Mg-1Mo	76 ± 6	273 ± 7	13.8 ± 0.7

Fig. 4. Stress-strain curve of monolithic Mg and Mo reinforced Mg nanocomposite tensile samples.

Fig. 5. Influence of nano Mo on the compressive properties of pure Mg.

The compressive testing results revealed that the addition of nano-sized Mo to Mg increased both yield and ultimate compressive strengths of magnesium matrix with a marginal decrease in the compressive failure strain as shown in Table 5. The nanocomposite containing 1 vol.% Mo particles showed the best compressive strength as shown in Fig. 5. The increase in compressive strength may be attributed to the particles associated with strengthening factors as indicated in the previous section. Interactions between twinning systems can also contribute to the increasing strength of Mg/Mo nanocomposites. Twinning develops actively new barriers to dislocations movement which is like grain size reduction. The formation of incoherent twin boundaries minimizes dislocations and possibly strengthens the composite. Marginal reduction in failure strain during compression loading may be attributed to
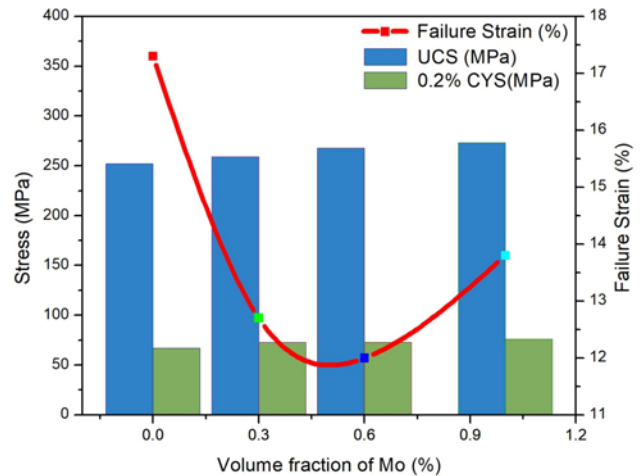
the increased capability of clusters to initiate new cracks.

3.3. Fracture behaviour

SEM examination of the fractured surfaces of the Mg-Mo nanocomposites under tensile loading revealed that under the far-field uniaxial tensile load, growth and coalescence of micropores and microcracks were observed as shown in Fig. 6. From the fractographs cleavage steps, dominated brittle failure is evident. The absence of enough slip system causes brittle failure in h.c.p. metals like magnesium [22]. A more significant number of microcracks are visible on the broken surface of Mg/Mo samples with an increasing amount of Mo due to the increasing presence of Mo particles clusters. The assortments of the microvoids were very random and irregular. The fractographs also indicated
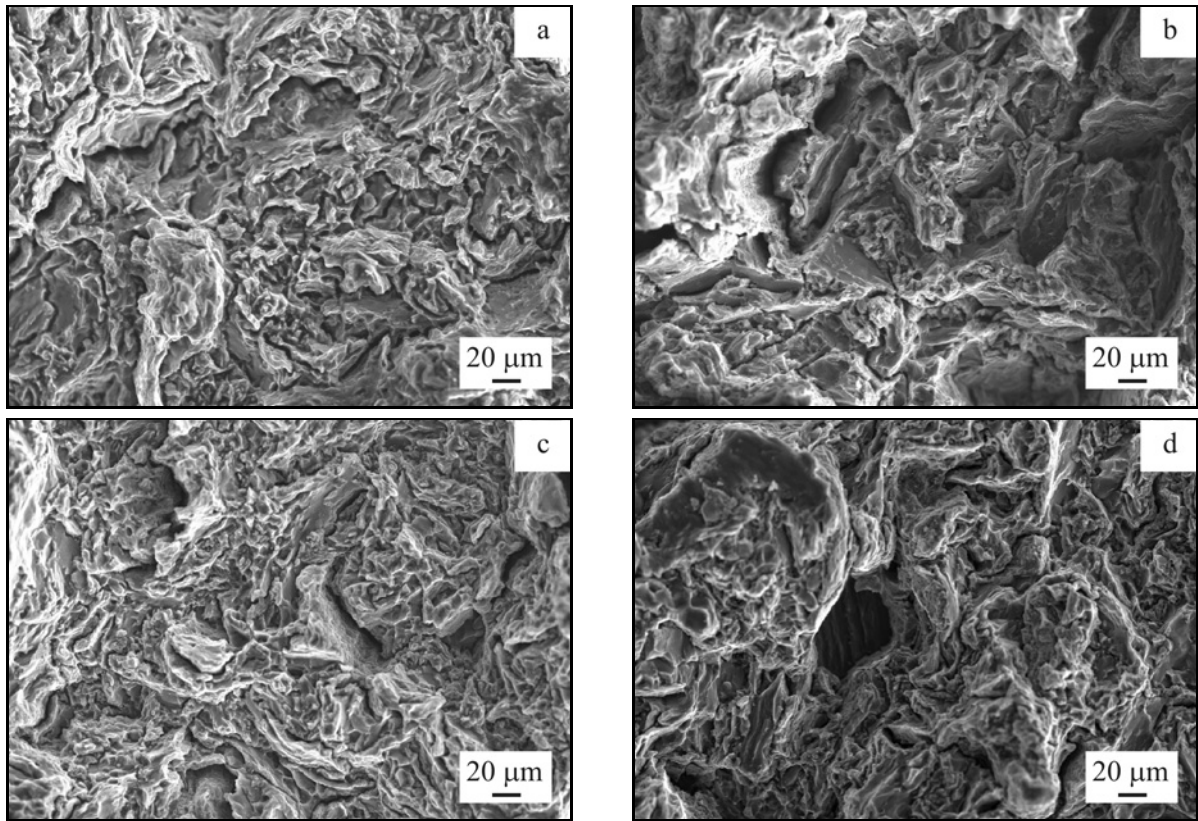
Fig. 6. SEM micrographs showing the broken surface of (a) pure Mg, (b) Mg/0.3Mo, (c) Mg/0.6Mo, and (d) Mg/1.0Mo composites under tensile loading.
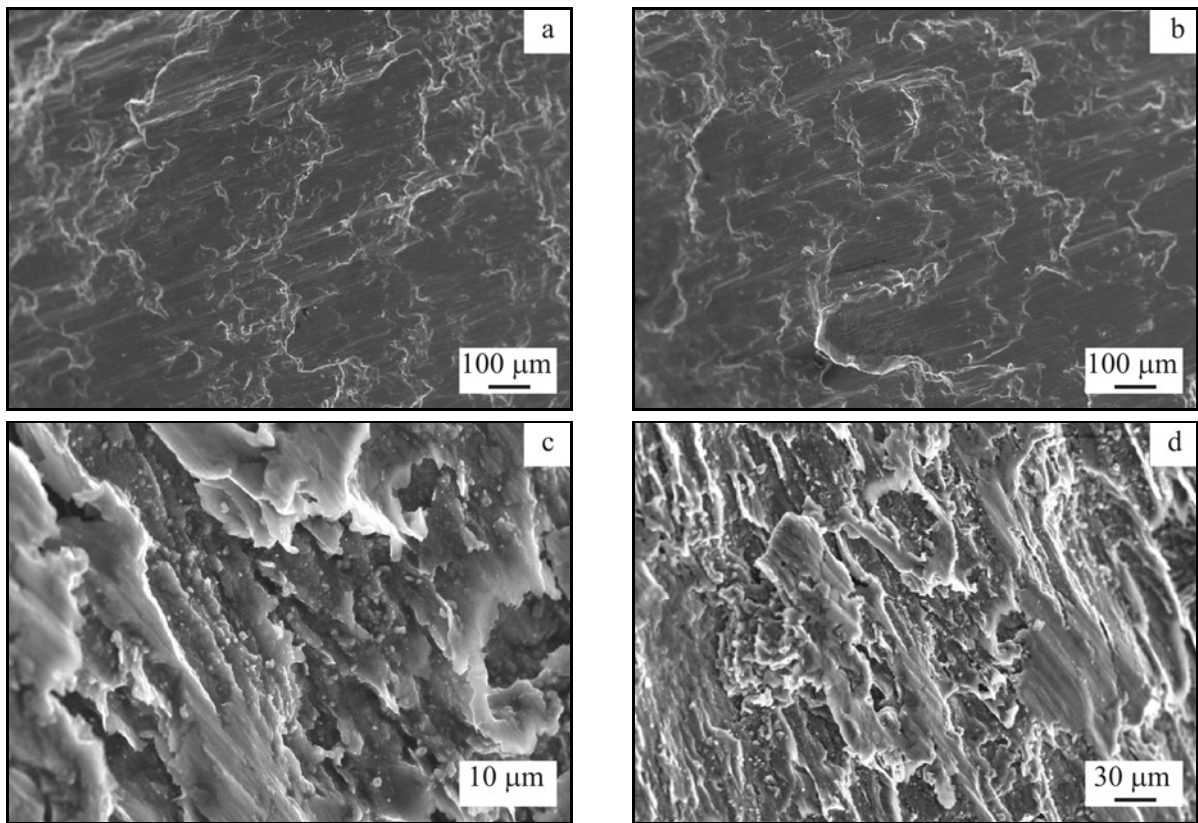

Fig. 7. SEM micrographs showing the broken surface of (a) pure Mg, (b) Mg/0.3Mo, (c) Mg/0.6Mo, and (d) Mg/1.0Mo composites under compressive loading.
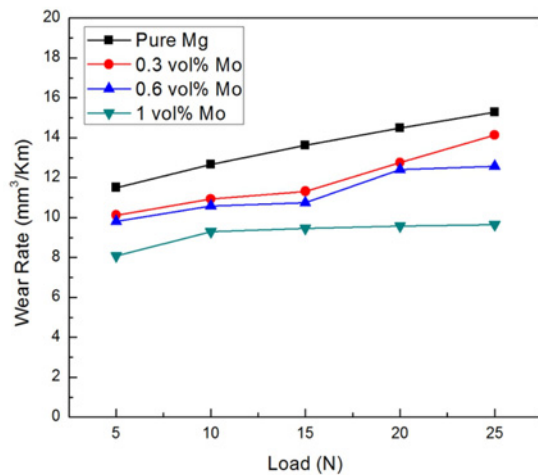
Fig. 8. Variation of wear rate as a function of normal load for the Mg-Mo composites.

Fig. 9. Variation of wear rate as a function of normal load for the Mg-Mo composites.

the concentration of damage in the region of locally clustered micro-voids.

Shear bands were observed on the fractured surfaces of pure and reinforced nanocomposite samples subjected to the uniaxial compressive test when examined by SEM as shown in Fig. 7. The surface of pure Mg and Mg-0.3 Mo was relatively smoother when compared to that exhibited by Mg-0.6 Mo and Mg-1Mo. The shear bands are assumed to originate from unstable perturbations of the lattice orientation. In general, twinning is a dominant mode of plastic deformation observed in Mg and its composites and appears to be the reason for the occurrence of shear banding. The crack initiated with an angle $45°$ inclined to the compressive axis for all the samples. The nanocomposites were broken into more than two pieces with the same inclination. Comparable results on the uniaxial compressive fracture behaviour at room temperature have been observed earlier [23]. The fracture nucleated from extreme ends towards the middle of the samples.

3.4. Wear behaviour

Figure 8 displays the effect of applied load and the volume percentage of Mo on wear rate at a constant sliding velocity of $1.25 \, \mathrm{m \, sec^{-1}}$. The wear rates of composites increased as the applied normal load increased. A mild wear regime was observed at lower loads. The increase of load can support plastic flow and transfer of metal in the friction surface, and hence the wear rate increased. A substantial amount of transfer layer gets severely damaged leading to higher wear rate with the increase of normal load.

Moreover, the nanocomposite specimens exhibited significantly lower wear rates as the Mo content increased as seen from Fig. 9. The reduction in wear rate can be attributed to the fact that the hard Mo
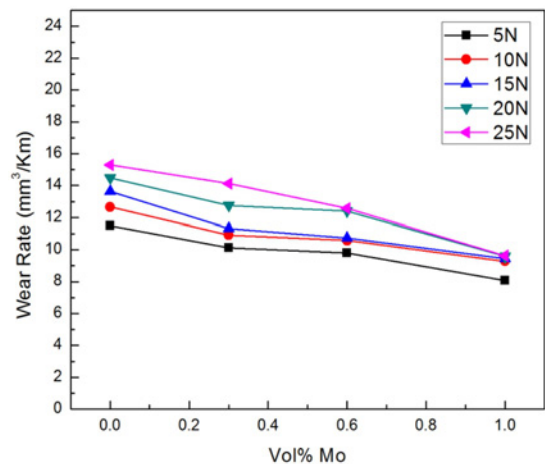
particles in composites offer to restrain to plastic deformation during friction and wear. For wearing bodies, the wear loss can often be assessed based on generalized Archard's wear model, which suggests that wear loss is directly proportional to the normal load and the sliding distance, but inversely proportional to the hardness of the material [24]. It is worthy of remarking this substantial reduction in wear rate under dry sliding condition was due to the relatively higher hardness of the nanocomposites.

The SEM micrographs obtained from the worn surface of the composite specimens are shown in Fig. 10. The results revealed that in many instances of material displacement to the sides causes the presence of many fine ploughing grooves. These grooves were parallel to the direction of sliding and suggestive of abrasive wear. The pattern of fine grooves was initially produced in pin surface by the significant effect of hard rigid reinforcements in between the sliding surfaces and can still plough through the surface of the pin. In general, the harder particulate reinforcements stand proudly on the surface of the soft matrix chip volume of material from the deep wear grooves [25]. At higher applied loads the depth of penetration of the grooves was likely to be more. Oxidized particles that detached from the contact surfaces trapped under the sliding pin dragged along the direction of sliding, probably leading to abrasive wear. In addition to these, many other micrometre-scale protruding surface irregularities can cause abrasive wear. Comparable results are generally observed when an abrasion phenomenon appears at the low normal load, followed by a corresponding increase in specific wear rate and the frictional coefficient. The presence of steel strip debris (Fig. 11) discarded on the worn surface indicates the considerable influence of abrasion as the dominant wear mechanism.
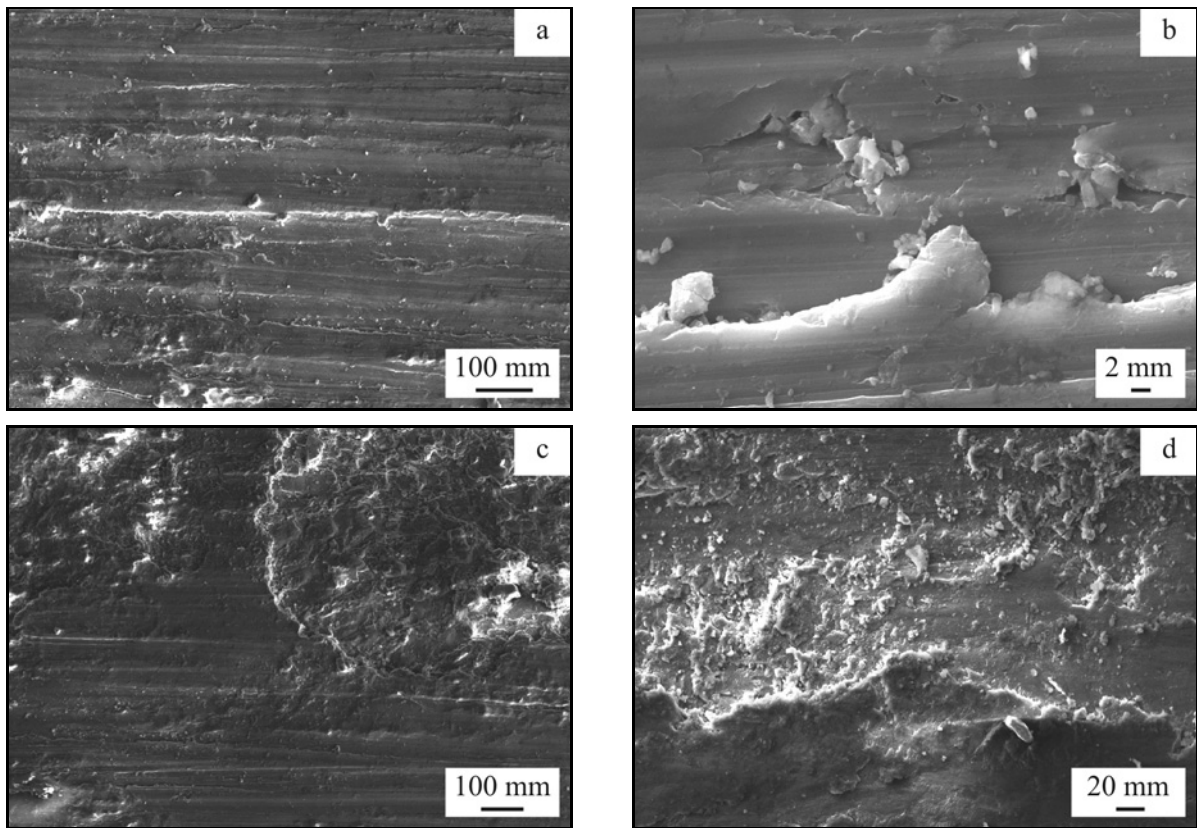
Fig. 10. SEM micrographs of the worn surfaces of pins tested at 1.25 m s^{-1}: (a), (b) 20 N; (c), (d) 25 N.
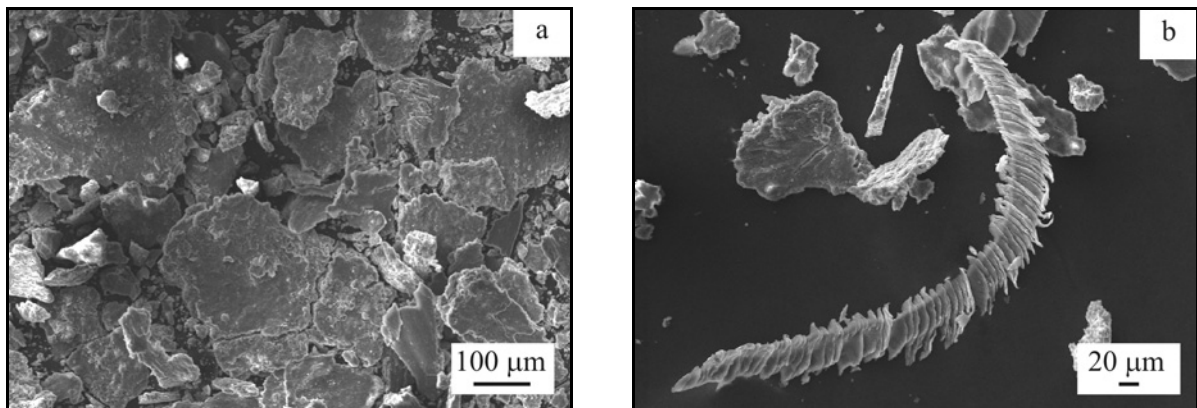

Fig. 11. SEM micrographs of the (a) wear debris and (b) steel strip debris.

At higher loads exceeding 15 N and reaching 25 N, however, the occurrence of severe scratches and shallow craters on the worn surface parallel to the direction of sliding indicates the delamination wear. From the geometrical characteristics and morphology of wear debris generated from dry sliding wear test, the hard Mo particles may emerge as constraints that enhance the resistance to plastic flow which indicates that delamination has occurred along the direction of sliding. It was also noted, through SEM analysis, the presence of lamellar wear debris (Fig. 11) that is often attributed to delamination.

The appearance of the worn surfaces involving oxidation products indicates typical oxidative wear. At loads higher than 10 N the frictional heat during sliding generates oxidative wear. Oxide films and metallic particles are retained on the worn surfaces, fill the grooves, act as a lubricating barrier and hence reduce the wear rate.

When Mg-based materials are subjected to dry sliding wear test against hardened steel disc surface, adhesive wear mechanism also predominates. The worn surfaces had matrix removal and slender paralleled furrows along the direction of sliding indi-

cating that these surfaces are subjected to observable adhesion phenomenon. These furrows gradually grew shallower. A separation event occurred on the worn surface of the composite with a higher amount of Mo indicating the adhesive wear mechanism.

4. Conclusions

Nano-sized molybdenum particles reinforced magnesium nanocomposites can be made by microwave assisted powder metallurgy route followed by hot extrusion. Reasonably uniform distribution of Mo particles with the limited presence of clusters indicates the suitability of processing parameters. The mechanical properties investigations revealed an improvement in mechanical attributes (hardness, tensile, and compressive strengths) with the loss of failure strain. Tensile fractographs exhibited the presence of micropores and microcracks, and the compressive fractographs showed the presence of shear bands. Dry sliding wear studies displayed a decline in wear rate (improved wear resistance) with the addition of Mo content. The principal wear mechanisms found at the surfaces included abrasion, delamination, adhesion, and oxidation.

References

[1] Augustyniak, A., Ming, W.: Progress in Organic Coatings, *71*, 2011, p. 406. doi:10.1016/j.porgcoat.2011.04.013

[2] Mallick, A., Tun, K. S., Gupta, M.: Materials Science and Engineering A, *551*, 2012, p. 222. doi:10.1016/j.msea.2012.04.116

[3] Hassan, S. F., Gupta, M.: Materials Research Bulletin, *37*, 2002, p. 377. doi:10.1016/S0025-5408(01)00772-3

[4] Wong, W. L. E., Gupta, M.: Composites Science and Technology, *67*, 2007, p. 1541. doi:10.1016/j.compscitech.2006.07.015

[5] Zhong, X. L., Wong, W. L. E., Gupta, M.: Acta Materialia, *55*, 2007, p. 6338. doi:10.1016/j.actamat.2007.07.039

[6] Hassan, S. F., Gupta, M.: Journal of Alloys and Compounds, *345*, 2002, p. 246. doi:10.1016/S0925-8388(02)00413-9

[7] Sanjay Kumar, T., Srivatsan, T. S., Gupta, M.: Materials Science and Engineering A, *466*, 2007, p. 32. doi:10.1016/j.msea.2007.02.122

[8] Wong, W. L. E., Gupta, M.: Advanced Engineering Materials, *7*, 2005, p. 250. doi:10.1002/adem.200400137

[9] Gupta, M., Wong, W. L. E.: Materials Characterization, *105*, 2015, p. 30. doi:10.1016/j.matchar.2015.04.015

[10] Gupta, M, Sharon, N., Mui, L.: Magnesium, Magnesium Alloys, and Magnesium Composites. New York, John Wiley & Sons 2011.

[11] Jäger, A., Lukáč, P., Gärtnerová, V., Haloda, J., Dopita, M.: Materials Science and Engineering A, *432*, 2006, p. 20. doi:10.1016/j.msea.2006.06.070

[12] Laser, T., Nürnberg, M. R., Janz, A., Hartig, Ch., Letzig, D., Schmid-Fetzer, R., Bormann, R.: Acta Materialia, *54*, 2006, p. 3033. doi:10.1016/j.actamat.2006.02.039

[13] Qi, W. H., Wang, M. P.: Journal of Materials Science Letters, *21*, 2002, p. 1743. doi:10.1023/A:1020904317133

[14] Kang, Y. C., Chan, S. L. I.: Materials Chemistry and Physics, *85*, 2004, p. 438. doi:10.1016/j.matchemphys.2004.02.002

[15] Ma, Z. Y., Tjong, S. C., Li, Y. L., Liang, Y.: Materials Science and Engineering A, *225*, 1997, p. 125. doi:10.1016/S0921-5093(96)10870-4

[16] Goh, C. S., Wei, J., Lee, L. C., Gupta, M.: Acta Materialia, *55*, 2007, p. 5115. doi:10.1016/j.actamat.2007.05.032

[17] Kubota, K., Mabuchi, M., Higashi, K.: Journal of Materials Science, *34*, 1999, p. 2255. doi:10.1023/A:1004561205627

[18] Suryanarayana, C.: Progress in Materials Science, *46*, 2001, p. 1. doi:10.1016/S0079-6425(99)00010-9

[19] El-Kady, O., Fathy, A.: Materials and Design, *54*, 2014, p. 348. doi:10.1016/j.matdes.2013.08.049

[20] Sevik, H., Kurnaz, C. S.: Materials and Design, *27*, 2006, p. 676. doi:10.1016/j.matdes.2005.01.006

[21] Hassan, S. F., Gupta, M.: Journal of Alloys and Compounds, *429*, 2007, p. 176. doi:10.1016/j.jallcom.2006.04.033

[22] Serra, A., Bacon, D. J., Pond, R. C.: Acta Materialia, *47*, 1999, p. 1425. doi:10.1016/S1359-6454(99)00016-6

[23] Nguyen, Q. B., Gupta, M.: Composites Science and Technology, *68*, 2008, p. 2185. doi:10.1016/j.compscitech.2008.04.020

[24] Archard, J.: Journal of Applied Physics, *24*, 1953, p. 981. doi:10.1063/1.1721448

[25] Colaço, R., Vilar, R.: Wear, *254*, 2003, p. 625. doi:10.1016/S0043-1648(03)00185-6 .